# Estimating orbital debris mass via solar radiation pressure and photometric signatures

**Jim Shell, PhD**
*Novarum Tech LLC*

## ABSTRACT

Mass is a fundamental attribute of resident space objects. For objects of known pedigree—specific rocket bodies or satellite bus types—the mass is usually well understood. However, for objects of unknown origin, to include orbital debris, there are few ready means of estimating object mass via remote sensing techniques. Estimating the debris mass from fragmentation events provide insight into the root causes and symmetry of these events by considering the conservation of momentum. Mass estimates of debris also enable an understanding if similar failure mechanisms were responsible for debris-generating events from common object types. Finally, understanding the mass of objects directly translates into the kinetic energy and an understanding of collision consequences.

Maturing an ability to estimate mass from readily available observational data and astrodynamic properties is a valuable technique as it may be applied to the space object population at scale. Historical techniques have predominantly focused on deriving non-conservative force components from propagation perturbations resulting from drag and solar radiation pressure. These non-conservative force components enable an estimation of an object's area-to-mass ratio. In turn, the signature of objects provides a size estimate of these objects. Taken together, a mass estimate is made possible.

Many mass estimation efforts have focused on low earth orbit objects where radar cross section and drag energy losses may be leveraged to estimate object mass. However, there are now space object catalogs such as the JSC Vimpel catalog, which contain numerous high-altitude objects and the explicit inclusion of area-to-mass estimates coupled with optical signatures. High perigee objects with negligible drag enable improved area-to-mass determination from the solar radiation pressure perturbations. Given that an object albedo is constrained from zero (fully absorptive) to one (fully reflective) enables a range of area-to-mass estimates. Like the application of radar cross section to derive object sizes, photometric signature data may be processed to derive an effective object area based upon similar albedo constraints. From the area-to-mass derived from solar radiation perturbations and inferred optical size, a mass estimation technique is enabled for high altitude objects. The higher the area-to-mass of an object, the better the mass estimate fidelity.

The development of the technique will be provided, along with an examination of specific breakup events and what may be inferred from the mass distribution from individual debris objects. Uncertainties in the estimation process are also provided which may then be validated against some "truth" sources where the mass of some objects are reliably know.

Past fragmentation events are analyzed using this analytical approach, where specific mass distributions and trends are observed. These mass distributions, coupled with the kinematic analysis of energetic events such as breakups and hypervelocity impacts, reinforce breakup models and inform the root cause of energetic events. Three different Centaur V breakup events are explored in detail, with the mass distributions supporting a hypothesis that a common root cause event was responsible for all three events. These Centaur V events (2014-055B, 2009-047B, 2018-079B), occurring within a one year time period, are significant given their debris constitutes the most numerous population in geo-transfer orbit (GTO). The resulting debris mass estimates are commensurate with expectations, demonstrating a promising potential for the technique.

## 1. INTRODUCTION

The continued growth of the resident space object (RSO) population shows no sign of diminishing. The era of "megaconstellations" has just begun, and the orbital debris population also keeps expanding. There is an unprecedented demand for space surveillance sensors and processing to inform space domain awareness and space traffic management. Novel algorithms to derive RSO physical properties are needed.

Mass is a fundamental object property. Mass directly translates into an object's kinetic energy and when coupled with relative velocities between objects informs the nature of collisions when they occur. For objects positively identified with known designs (e.g., a specific rocket body, a particular satellite bus), mass estimates are readily available. However, discerning the mass of unidentified objects and fragmentation debris not a trivial matter given the observational data which are available.

This work explores the coupling between the non-conservative forces manifested in orbit propagation and RSO signatures which is leveraged to provide RSO mass estimates. Specifically, the perturbations due to solar radiation pressure and the optical signature of objects is examined to demonstrate an approach for estimating and constraining the mass of RSOs.

## 2. SOLAR RADIATION PRESSURE AND OPTICAL SIGNATURES

Solar radiation pressure (SRP) arises from the interaction of the sun's electromagnetic radiation upon an object. SRP results in a force on all objects, and this force must be accommodated for accurate propagation. For objects with perigee heights > 800 km, SRP is the dominant non-conservative force (with drag being the dominant non-conservative force for lower altitudes) [1]. The larger the area of the object, the higher the resulting SRP force. The acceleration, in turn, is higher for lower mass objects. A cursory review of this force is provided.

What better place to begin than Newton's second law, colloquially represented as the force ($F$) being equal to the product of mass ($m$) and acceleration ($a$),

$$F = ma.$$

When a pressure is applied, such as SRP, the force is obtained by the product of the pressure ($P$) and the surface area ($A$) over which the pressure is applied or

$$F = PA.$$

Equating the two forces results in

$$ma = PA,$$

or solving for acceleration as

$$a = \frac{PA}{m}$$

So what is the magnitude of this pressure resulting from solar radiation? The SRP results from photon momentum transfer to the object which is under illumination. At Earth's distance from the sun, and for a completely absorbing material, the SRP is approximately $P_{sr} = 4.57\ uN/m^2$. To help provide a more intuitive reference point, consider a typical garden ant which has a mass of 2 mg, or ~ 20 uN. So, the solar radiation pressure is similar to the weight of an ant distributed over 4 square meters or ~ 43 square feet.

This pressure is also a function of how reflective an object is. Any reflection of the solar radiation adds additional pressure akin to an elastic collision in mechanics. The total pressure is therefore

$$P = P_{sr}\ C_\rho$$

where $C_\rho$ is the reflectivity coefficient. The reflectivity coefficient is in turn defined as

$$C_\rho = 1 + \rho$$

where $\rho$ is the reflectivity of an object, or albedo. This term is better appreciated if one considers classical mechanics interactions which range from completely inelastic to fully elastic. The inelastic case imparts the least force and is when the reflectivity is zero. The elastic case is the extreme opposite in which there is total reflection, resulting in a doubling of the force.[1]

Given this development, the acceleration of an object due to SRP may be expressed as

$$a = \frac{P_{sr}\, C_\rho\, A}{m} \qquad Eq\ \ 1$$

From this equation it is observed that SRP acceleration is a function of three independent variables: the projected area to the sun ($A$), the reflectivity ($\rho$), and the mass ($m$). The kinematic motion of an orbiting object is only concerned with the net acceleration; thus no insight is provided into the relative values of these three independent variables.

However, some constraints are present. The reflectivity, $\rho$, is bound to the range of [0 1]. For most objects, in particular inactive objects not expending propellant, the mass remains fixed. However, the effective projected area or area * albedo product can vary meaningfully. These variations arise from both darkening of materials over time lowering the net reflectivity (commonly observed in aging rocket bodies), but it also includes the changing projected area of debris objects having rotational angular momentum and presenting distinct geometries over an annual cycle.

Historically, the product of the area/mass and the reflectivity coefficient have been termed "AGOM," from an early paper in which the variables representing the acceleration were Area Gamma Over Mass.[2] It is only the AGOM value that may be determined from the orbit fitting process. However, it is common practice to simply refer to the area-to-mass ratio (A/m) of an object. These references will often assume a constant reflectance (often $\rho$ = 0.1 or 0.2).

$$AGOM = \frac{C_\rho\, A}{m}$$

Thus far, only scalar values have been presented, but the world is not so simplistic. To first order, the SRP acceleration is in a direction opposite the sun as anticipated. However, the complexity of object shapes, rotational states, and the detailed reflective properties or BRDF (bidirectional reflectance distribution function) of various materials all interplay to create many nuances. Nevertheless, a simple "cannonball" model for SRP will be assumed for this effort.

The magnitude of the SRP acceleration relative to others experienced by an orbiting object is illustrated in Figure 1. The relative magnitude directly relates to the uncertainty for the AGOM estimate. At geosynchronous altitudes, the SRP acceleration magnitude for a typical satellite or rocket body (area/mass ~ 0.01-0.03 $m^2$/kg) is approximately two orders of magnitude less than the J2 perturbations due to earth's oblateness. However, for debris objects, it is not uncommon to have an area/mass of 1.0 $m^2$/kg (or higher), which results in such objects experiencing an acceleration from SRP commensurate with the J2 perturbation (which, as seen in the figure, is also comparable to lunar effects at geosynchronous altitudes).

[1] Strictly speaking, $C_\rho$ can range from 0 to 2. If a material is transmissive, then the reflectivity value may effectively become negative.

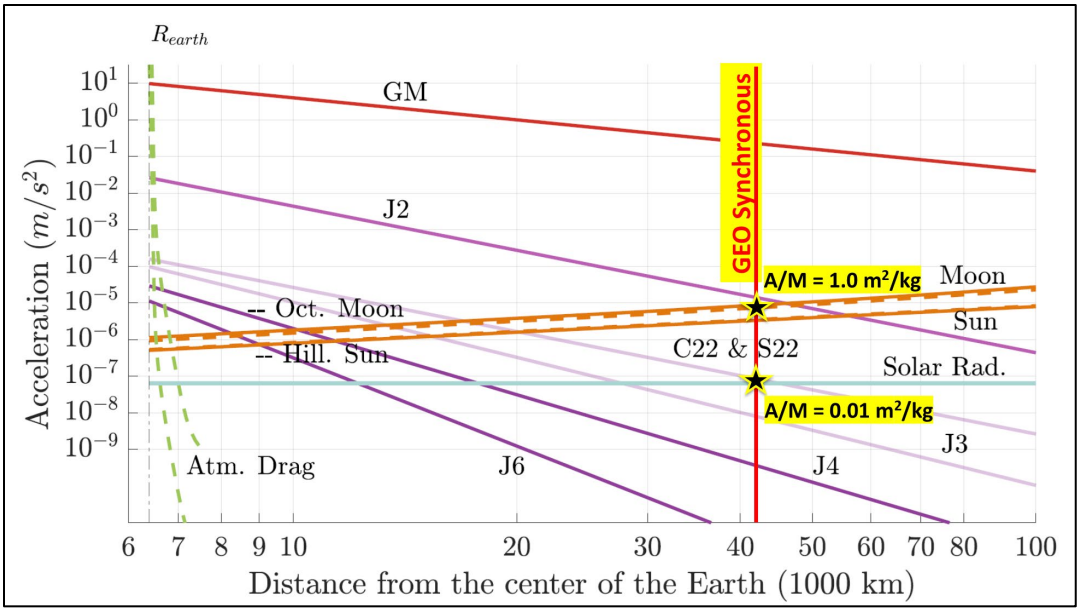


*Figure 1 The magnitudes of perturbing accelerations on orbiting objects. At geosynchronous altitudes, a typical satellite or rocket body (with area/mass ranging from 0.01 – 0.03 m²/kg) is perturbed at 1/100 the magnitude of lunar forces and J2. However, for higher area/mass objects the SRP force becomes commensurate with lunar and J2. Modification of figure courtesy of Wu and Rosengren[3] (Creative Commons Attribution 4.0 License).*

Attention is now turned to the optical signatures of RSOs. Photometric data from optical sensors may be used to model the brightness of an object over various geometric conditions, and in turn used to estimate the area*albedo product. The source of data used here is from the JSC Vimpel catalog which fits photometric data to a diffuse sphere phase function coupled with a range normalization to 40,000 km. The equation for the visual magnitude ($m_v$) of a diffuse sphere of area ( $A_{opt}$), at given solar phase angle of ∅, and at a range of $R$ is given as

$$m_v = m_{sun} - 2.5\log\left[\frac{\rho\, A_{opt}}{R^2} F(\emptyset)\right]$$

As both reflectance and area appear in the equation for solar radiation pressure, these terms are solved for resulting in

$$\rho\, A_{opt} = \left[\frac{R^2}{F(\emptyset)}\right] 10^{0.4(m_v - m_{sun})} \qquad Eq\ 2$$

Having obtained the reflectivity * area (albedo * area) product, this term may now be combined with the AGOM component to produce the sought-after mass estimate.

$$m = \frac{\rho\, A_{opt}}{(1+\rho)\left(\frac{A}{m}\right)_{srp}} \qquad Eq\ 3$$

Here the *srp* subscript denotes this value is obtained by the computed AGOM due to fitting orbit perturbations.

Figure 2 provides an empirical example of an object where the mass is known to have been held constant, but the values of the numerator (optical signature) and denominator (AGOM) change in tandem.

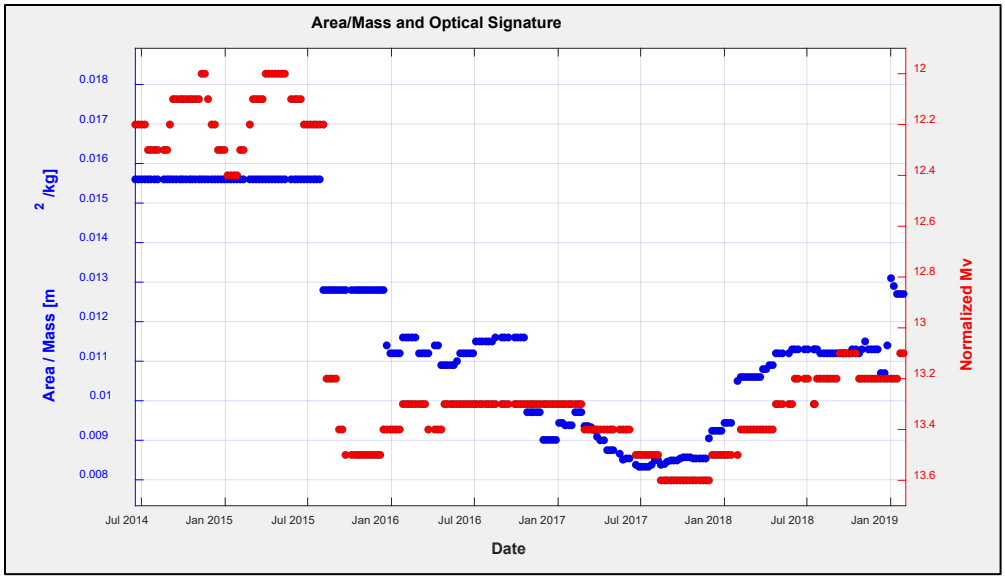


*Figure 2 The coupling between the area/mass (left axis) and the optical signature (right axis) is readily apparent in this example of a 3-axis geosynchronous satellite which has ceased operating (data from JSC Vimpel catalog, object #143600 [4]). Upon becoming inactive, the satellite stops maintaining solar array pointing toward the sun, decreasing the projected area. This in turn also results in a net decrease in the optical signature due to the reduced illumination area.*

## 3. DEBRIS CHARACTERISTICS

It's appropriate to briefly review the nature of the orbital debris population. There is a large population of higher area/mass ratio (so called "HAMR") objects which persist in HEO and GEO region orbits [5, 6]. Growing consensus attributes these objects to multi-layer insulation or thermal control blankets which have degraded over time and "sloughed" off their hosts, often with their origin near the geosynchronous region. Impacts by small micrometeoroids or untracked space debris may similarly liberate these objects from their hosts. When such HAMR objects originate from low earth orbit (LEO) objects, their lifetimes are naturally limited due to the drag as well as solar radiation perturbations which increase the orbital eccentricity, in turn lowering the perigee height to a sufficient degree that drag cleanses these objects from the orbit.

There are few reliable sources from which HAMR object states and properties may be gleaned. The public domain US catalog contains few qualifying objects, in part due to the prerequisite of identifying the parent object from which the debris originated. However, the Russian JSC Vimpel catalog [7] provides an excellent source which may be leveraged to better understand and research the attributes of such objects. The data presented hereafter is taken from the JSC Vimpel space object catalog. Objects in the Vimpel catalog have been verified via tracking with commercial electro-optical sensors, with their attributes consistent with that published by Russia (where the attributes in question are the area/mass values and optical signatures).

## 4. ANALYSIS OF DEBRIS EVENTS

Attention is now turned to specific debris-generating events for which the mass estimation technique may be applied. There are three events involving Atlas V Centaur upper stages which are of particular interest due to the numerous fragments produced and the high perigee heights such that solar radiation pressure is by far the most dominant non-conservative force, thus enabling more accurate estimates of AGOM or area/mass. These three events also occurred within an eight-month span, and presumably may have had the same root cause. Finally, the uniqueness of the parent object orbits enables high-confident assignment of debris objects sourced to these events. A summary of the events is provided in Table 1.

*Table 1 Three Atlas V Centaur rocket bodies fragmented over a relatively short duration in late 2018 and early 2019. The debris generated constitute an ideal data set to examine the mass properties exploiting the solar radiation pressure and optical signature.*

| Catalog Object (COSPAR / NORAD) | Fragmentation Date | US Catalog Fragments as of Sep 1, 2023 | Vimpel Catalog Fragments |
|---|---|---|---|
| 2014-055B / 40209 | August 30, 2018 | 109 (24 "lost"[2]) | > 500 |
| 2009-047B / 35816 | March 24, 2019 | N/A | > 600 |
| 2018-079B / 43652 | April 06, 2019 | 214 (74 "lost") | > 800 |

Comparison between the US NORAD (space-track.org) and JSC Vimpel catalogs is not an equitable comparison. To first order, the state quality and pedigree of objects in the US catalog is significantly better than that of the Russian Vimpel catalog. However, the Vimpel catalog has a much more complete object count and provides object properties unavailable in the US catalog (e.g., object area/mass, visual magnitude, state error metrics). Finally, there are no debris fragments in the US catalog from the 2009-047B rocket body, but the event was widely observed by the international community [8, [9]].

The Vimpel catalog does not provide object identification. It is therefore necessary to analyze these events and determine from the statistics of the joint orbital parameters which objects originated from the specific event. Early in each of the events, it was possible to directly correlate the debris field objects to the parent object. Using these objects as a "truth" set, the evolution of the orbital elements may be used to establish the current population. As stated earlier, the uniqueness of each of these orbits enables a successful accounting of these objects without introduction of false positive members. A summary of the orbit elements of each debris field is provided in Table 2.

*Table 2 The primary orbital elements of the debris fields for each of the Atlas V Centaur breakups as of June 5, 2023.*

| Catalog Object (COSPAR / NORAD) | Semi-major axis & standard deviation [km] | Inclination & standard deviation [deg] | RAAN & standard deviation [deg] | Eccentricity & standard deviation |
|---|---|---|---|---|
| 2014-055B / 40209 | 28091 ± 1017 | 20.63 ± 0.44 | 248.0 ± 32.7 | 0.486 ± 0.052 |
| 2009-047B / 35816 | 27070.0 ± 19.4 | 24.10 ± 0.17 | 316.45 ± 1.40 | 0.515 ± 0.010 |
| 2018-079B / 43652 | 28158 ± 1917 | 11.43 ± 1.23 | 127.9 ± 7.9 | 0.469 ± 0.047 |

The Vimpel catalog contains numerous objects from these events which have not been tracked for an extended duration (> 6 months) and as such the state accuracy is significantly degraded. Given the state errors and large population of objects which have not been updated, a constraint was placed on requiring an in-track accuracy estimate of 1000 km (supplied by Vimpel) to help ensure objects are not double counted and indeed unique. The results of this exercise produced the following object population from which the mass analyses proceeded:

- 2014-055B 315 objects
- 2009-047B 191 objects
- 2018-079B 548 objects

[2] "Lost" is a designation for objects which have not been tracked in the last 30 days, and as such are precluded from conjunction analysis by USSPACECOM.

*Figure 3 An Atlas V Centaur upper stage (single engine variant) [10]. The stage has a diameter of 3.05 m, and length of 12.68 m to include the nozzle, and an inert mass of 2,243 kg with the primary tank comprised of stainless steel 20 mils (~51 mm) thick.*

## 5. RESULTS

Examination of these three debris events via Eq 3 is presented. Figures 4-6 provide a summary of each event by illustrating the distributions of mass, area/mass, visual magnitude, and finally the joint area/mass-visual magnitude. The reflectivity ($\rho$) was allowed to vary between 0.05 and 0.60, providing a range of mass estimates per Eq 3.

While there are many uncontrolled variables in this analysis (e.g., the subset of the object populations with reasonable states), the brighter pieces are tracked with more regularity and to first order would be representative of the largest mass fraction of the total debris population.

*Table 3 Estimated total debris mass from each of the three Atlas V Centaur upper stage events.*

| Catalog Object (COSPAR / NORAD) | Total Debris Mass Estimate $\rho = 0.05$ | Total Debris Mass Estimate $\rho = 0.60$ |
|---|---|---|
| 2014-055B / 40209 | 395 kg | 259 kg |
| 2009-047B / 35816 | 226 kg | 148 kg |
| 2018-079B / 43652 | 456 kg | 299 kg |

Given the parent object mass of ~2200 kg, the mass estimates seem reasonable. Examination of the area/mass distributions per Figures 4-6 reveal a bimodal distribution observed in other events.

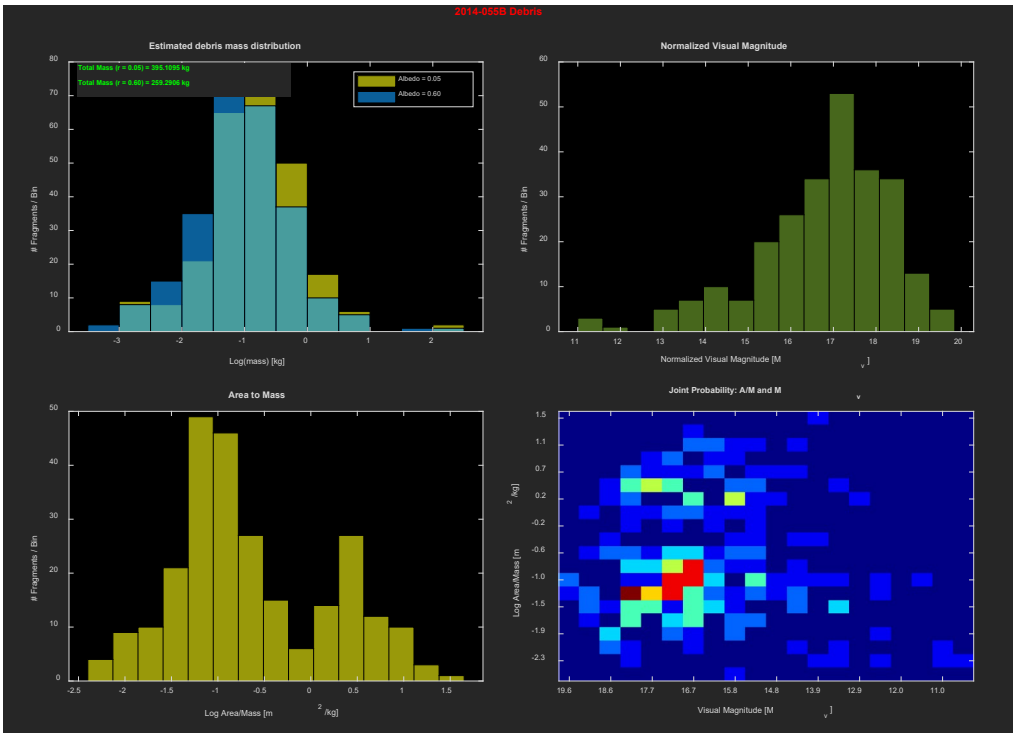


*Figure 4 Summary of the 2014-055B Atlas V Centaur upper stage debris objects. Object mass distribution (top left), normalized visual magnitude distribution (top right), area/mass distribution (bottom left), and joint distribution of area/mass and normalized visual magnitude.*

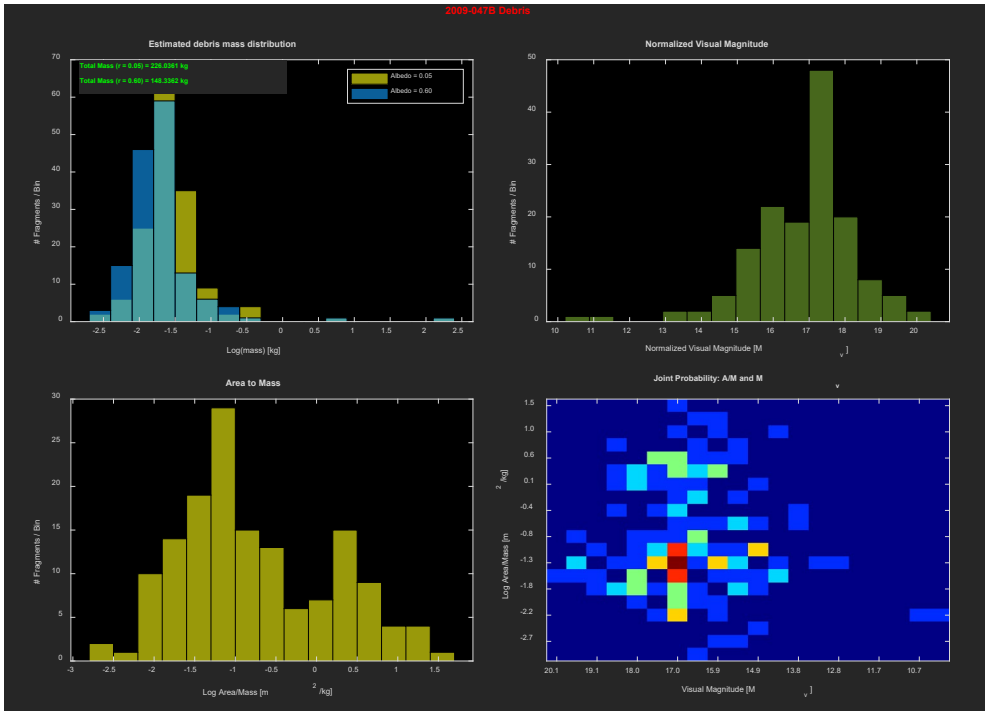


*Figure 5 Summary of the 2009-047B Atlas V Centaur upper stage debris objects. Object mass distribution (top left), normalized visual magnitude distribution (top right), area/mass distribution (bottom left), and joint distribution of area/mass and normalized visual magnitude.*

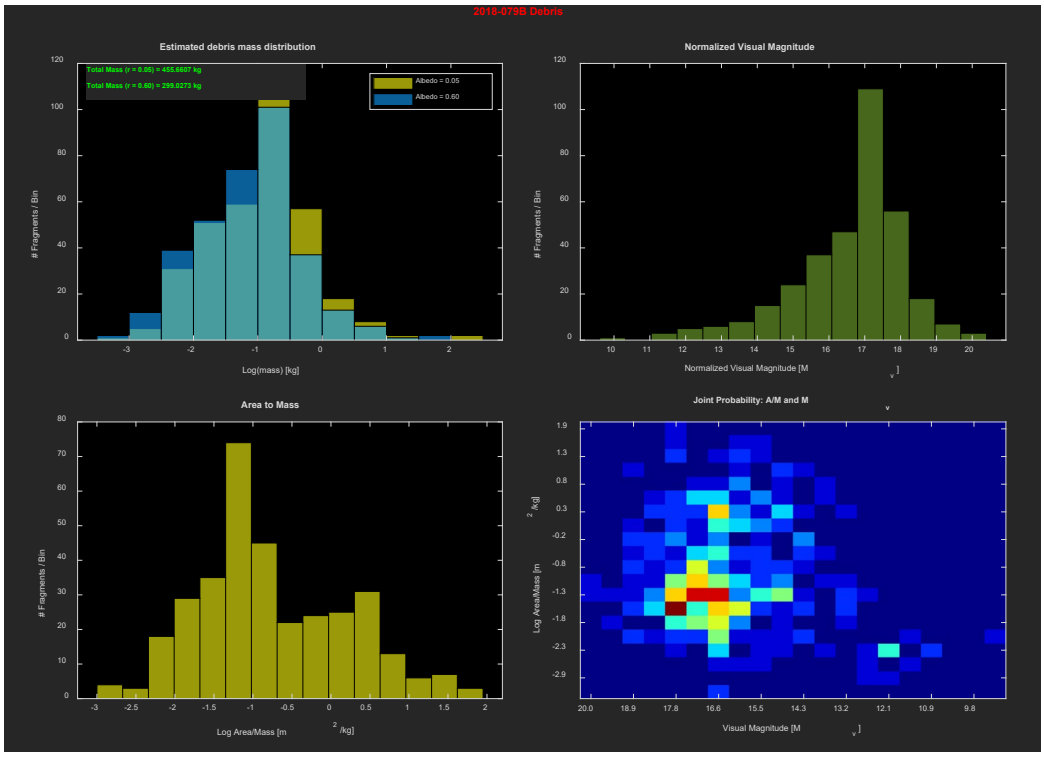


*Figure 6 Summary of the 2018-079B Atlas V Centaur upper stage debris objects. Object mass distribution (top left), normalized visual magnitude distribution (top right), area/mass distribution (bottom left), and joint distribution of area/mass and normalized visual magnitude.*

## 6. SUMMARY AND FUTURE WORK

A technique to estimate the mass of resident space objects has been developed leveraging perturbations due to solar radiation pressure coupled with the photometric signatures of objects. Analysis of three specific events suitable for this analysis produced results commensurate with expectations.

Future work should examine the mass uncertainties resulting from AGOM estimate errors, in particular for lower area/mass objects where the perturbing force of the solar radiation pressure is minimal in comparison to other perturbations.

## BIBLIOGRAPHY

[1] Vallado, David A., "Fundamentals of Astrodynamics and Applications," 4th edition, 2013 Microcosm Press.

[2] Hejduk, M.D. and R.W. Ghrist, "Solar Radiation Pressure Binning for the Geosynchronous Orbit," AAS 11-581, https://ntrs.nasa.gov/api/citations/20110015238/downloads/20110015238.pdf, accessed August 2023.

[3] Wu, Di and Aaron Rosengren, "An investigation on space debris of unknown origin using proper elements and neural networks," https://assets.researchsquare.com/files/rs-2432104/v1/e989d4a48423c2c5fc52d1ab.pdf accessed August 2023.

[4] JSC Vimpel space object catalog. http://spacedata.vimpel.ru/, accessed August 2023.

[5] Schildknecht, T., et al, "Optical Observations of Space Debris in High-altitude Orbits," *Proceedings of the Fourth European Conference on Space Debris*, Darmstadt, Germany, 18-20 April 2005, (ESA SP-587, August 2005).

[6] Liou, J.-C. and J.K Weaver, "Orbital Dynamics of High Area-to-mass Ratio Debris and Their Distribution in the Geosynchronous Region," *Proceedings of the Fourth European Conference on Space Debris*, Darmstadt, Germany, 18-20 April 2005, (ESA SP-587, August 2005).

[7] JSC Vimpel space object catalog. http://spacedata.vimpel.ru/, accessed August 2023.

[8] Molotov, I. E., et al, "Russian-Chinese Observations of Fragments of the Destruction of the Centaur Rocket Stage are the First Step to the Network of BRICS Observatories," All-Russian Scientific Conference with International Participation Space Debris: Fundamental and Practical Aspect of the Threat, Moscow, April 17–October 19, 2019 http://dx.doi.org/10.21046/spacedebris2019-95-102 accessed August 2023.

[9] "Rocket break-up provides rare chance to test debris formation," European Space Agency, https://www.esa.int/Space_Safety/Rocket_break-up_provides_rare_chance_to_test_debris_formation accessed August 2023.

[10] NASA Image and Video Library, https://images.nasa.gov/details-KSC-20210715-PH-RNB01_0132 accessed August 2023.